The local field distribution of Gd^{3+} in transition metal fluoride glasses investigated by electron paramagnetic resonance

1996 J. Phys.: Condens. Matter 8 4339

(http://iopscience.iop.org/0953-8984/8/23/023)

J. Phys.: Condens. Matter **8** (1996) 4339–4350. Printed in the UK

The local field distribution of Gd^{3+} in transition metal fluoride glasses investigated by electron paramagnetic resonance

C Legein†, J Y Buzaré‡, G Silly‡ and C Jacoboni†

† Laboratoire des Fluorures, URA CNRS 449, Faculté des Sciences, Université du Maine, 72017, Le Mans Cédex, France

‡ Laboratoire de Physique de l'Etat Condensé, URA CNRS 807 Faculté des Sciences, Université du Maine, 72017, Le Mans Cédex, France

Received 19 January 1996, in final form 21 March 1996

Abstract. The EPR spectra of Gd^{3+} in two transition metal fluoride glasses (PZG and PBI) have been extensively studied as functions of temperature, Gd^{3+} concentration and microwave frequency (S, X, K and Q bands). The marked changes observed in the EPR spectra with temperature and concentration imply the existence of pairs of Gd^{3+} ions. The spectra of isolated Gd^{3+} ions were obtained at low temperature for samples with low Gd^{3+} doping concentration. Isolated Gd^{3+} ions are characterized by a fine-structure b_2^0-parameter distribution within the range 0.02–0.15 cm^{-1}. The simulations of these spectra are computed with a Czjzek fine-structure parameter distribution (this solution prohibits the existence of axial symmetry sites). It indicates a decrease of the number of geometrical constraints compared to those for Cr^{3+} and Fe^{3+} (octahedral coordination in a fluoride medium), in agreement with the higher Gd^{3+} coordination numbers. Gd^{3+}-ion sites are found to be more distorted in PZG than in PBI, suggesting that the glass network has an influence on the Gd^{3+} polyhedron distortion amplitude.

1. Introduction

The purpose of the present study is to investigate the electron paramagnetic resonance (EPR) spectra of the S-state rare-earth ion Gd^{3+} in transition metal fluoride glasses (TMFG) as functions of glass composition, doping concentration, temperature and microwave frequency (S, X, K and Q bands), and to determine the distribution of the crystal-field parameters acting on Gd^{3+} in TMFG.

Although numerous studies have been devoted to Gd^{3+} spectra in amorphous compounds, only one of them dealt with their reconstruction [1]. The following spin Hamiltonian which incorporates the Zeeman and the crystal-field interactions (where terms of order higher than two are neglected) is used:

$$H = g\beta \boldsymbol{H} \cdot \boldsymbol{S} + \frac{1}{3}(b_2^0 O_2^0 + b_2^2 O_2^2) \tag{1}$$

with the following fine-structure parameter (b_2^0, $\lambda = b_2^2/b_2^0$) distributions: Gaussian for b_2^0 ($0.051 \leqslant (b_2^0)_{moy} \leqslant 0.056$ cm^{-1} and $0.017 \leqslant \Delta b_2^0 \leqslant 0.021$ cm^{-1}); and broad and slowly varying for λ with appreciable probability over the whole range $0.0 \leqslant \lambda \leqslant 1.0$ (figure 1). This fine-structure distribution leads to high probability values for axially symmetric sites ($\lambda = 0$).

0953-8984/96/234339+12$19.50

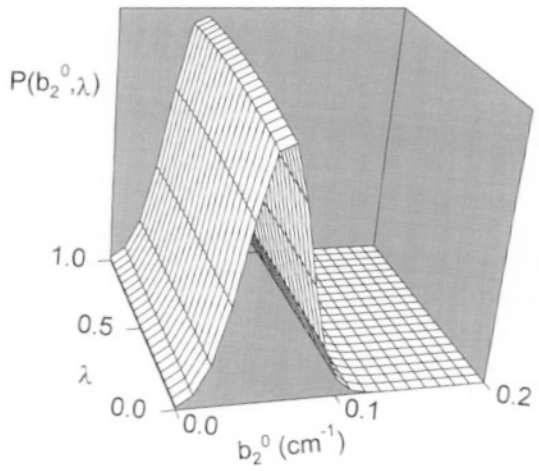

Figure 1. The fine-structure parameter distribution used by Brodbeck and Iton [1]: multiplication of two Gaussian functions with $(b_2^0)_{moy} = 0.056$ cm^{-1}, $\Delta b_2^0 = 0.019$ cm^{-1}, $\lambda_{moy} = 0.75$ and $\Delta\lambda = 2$ (λ_{moy} and $\Delta\lambda$ have been estimated; no analytical expression was given in [1]).

In a previous paper, we have shown that the following distribution of crystal-field parameters:

$$P(b_2^0, \lambda) = \left[1/\left((2\pi)^{1/2}\sigma^d\right)\right](b_2^0)^{d-1}\lambda(1-\lambda^2/9)\exp-\left[(b_2^0)^2(1+\lambda^2/3)/2\sigma^2\right] \qquad (2)$$

initially applied by Czjzek *et al* to the calculation of the electric field gradient in amorphous materials [2], allows one to take into account the essential features of Cr^{3+} and Fe^{3+} EPR spectra in TMFG and to reconstruct these spectra accurately [3]. The main difference from the above-mentioned distribution is that the function $P(b_2^0, \lambda)$ yields zero probability for both $b_2^0 = 0$ and $\lambda = 0$; the existence of high-symmetry polyhedra is prohibited, in agreement with the notion of disorder generally considered in glasses. Thus, this fine-structure parameter distribution $P(b_2^0, \lambda)$ was used to reconstruct the EPR spectra of the Gd^{3+} ions in TMFG. *Ab initio* simulations have also been achieved by applying distributions similar to those used by Brodbeck and Iton [1] in order to compare the efficiency of these two solutions.

In the distribution (2), σ and d are two adjustable parameters; σ characterizes the interaction force and d is the number of independent random components ($d \leqslant 5$) of the fine-structure tensor which can be expressed as a 3×3 symmetric traceless matrix, thus determined by five independent quantities (b_2^m; $m = 0, \pm1, \pm2$) for fully random disorder. Some local order implies an increase of geometrical constraints and consequently a decrease of the number of independent quantities. The d-value deduced from Cr^{3+} and Fe^{3+} EPR spectra simulation in TMFG, where octahedral coordination is plainly established for these ions, is $d = 3$ [3]. So, another interesting goal of this work is to test the influence of the coordination number on the d-value with Gd^{3+}, which is known to adopt a coordination number larger than six in a fluoride medium.

2. Experimental procedures

The EPR spectra were studied for TMFG derived from two basic glasses: PZG (35 PbF_2, 24 ZnF_2, 34 GaF_3, 5 YF_3, 2 AlF_3 (mol%)) [4] and PBI (19 PbF_2, 23 BaF_2, 47 InF_3, 2 AlF_3, 4.5 YF_3, 4.5 SrF_2 (mol%)) [5]. GdF_3 was added at different concentrations. After preliminary mixing, the melt was placed in covered platinum crucible and heated at 800 °C, and then cast into a preheated (200 °C) mould. Owing the fact that fluoride compounds are moisture sensitive, all preparative work was done inside a dry glove-box.

The X-band (9.5 GHz) and S-band (4 GHz) spectra were recorded on a Bruker spectrometer; measurements were achieved at variable temperature (X band) by using an Oxford cryostat. The K-band spectrometer (19 GHz) was designed and assembled in the IBM Zurich laboratory [6]. The Q-band spectrum (35 GHz) was recorded by P Simon in the CRPHT (UP CNRS 4212).

3. Gd^{3+} EPR spectra in TMFG

The rare-earth S-state ion, Gd^{3+}, in glassy hosts (phosphate [7, 8], borosulphate [9], oxy-halo borate [10], silicate [11–12], lead acetate [13], ZnF_2–BaF_2–RF_3 [8], fluorozirconate [14]) routinely exhibits an X-band EPR spectrum characterized by three prominent features with effective g-values of ∼5.9, 2.8 and 2.0. This spectrum is labelled the U spectrum because of its 'ubiquity' and Gd^{3+} ions are frequently suspected to impose their environment, when present as impurities in glass systems [9–11, 13, 15]. Nevertheless, examinations of the spectra exhibited in the above-mentioned articles show that the intensity ratios of the three prominent features change in going from one glassy system to another, and often with composition in a given glassy system [7–9, 11, 12]. Thus, Gd^{3+} ions seem to be sensitive to their environment in glasses. In TMFG, the intensity ratio of the three prominent features changes with glass composition, but also with temperature or doping concentration.

On reconstruction of Cr^{3+} and Fe^{3+} spectra, we noticed that different fine-structure parameter distributions, corresponding to different sets of σ- and d-values, allow us to provide similar calculated spectra for a given microwave frequency. Nevertheless, a simultaneous agreement at different frequencies was obtained with a single (σ, d) set [3]. Thus, the study of the microwave frequency dependence spectra is essential. It allows us to dispose of several spectra in order to determine the actual fine-structure parameter distribution acting on the paramagnetic ion.

In the following, we summarize the main features of the Gd^{3+} EPR spectra in TMFG versus temperature, doping concentration and microwave frequency.

3.1. Temperature and concentration dependence

At X band (figure 2), a broad line whose intensity increases with concentration and temperature is superimposed on a narrower one at $g = 2$. When temperature decreases, the increase of the amplitude ratio for the $g = 5.9$ to $g = 2$ peaks has been observed in oxide glasses [9, 12] and in zeolites [16]. Similar concentration and temperature dependences of the broad $g = 2$ line have been noted for Cr^{3+} and Fe^{3+} ions in TMFG. The observed spectra have been attributed to isolated paramagnetic ions and exchange-coupled pairs [17]. As for Cr^{3+} and Fe^{3+}, the broad line at $g = 2$ can also be attributed to exchange-coupled pairs of Gd^{3+} ions. As we are mainly interested in isolated ions, we have recorded Gd^{3+} EPR spectra at low temperature for samples with low Gd^{3+} doping concentration at X and K bands. Under these conditions, Gd^{3+} spectra can be attributed to isolated ions.

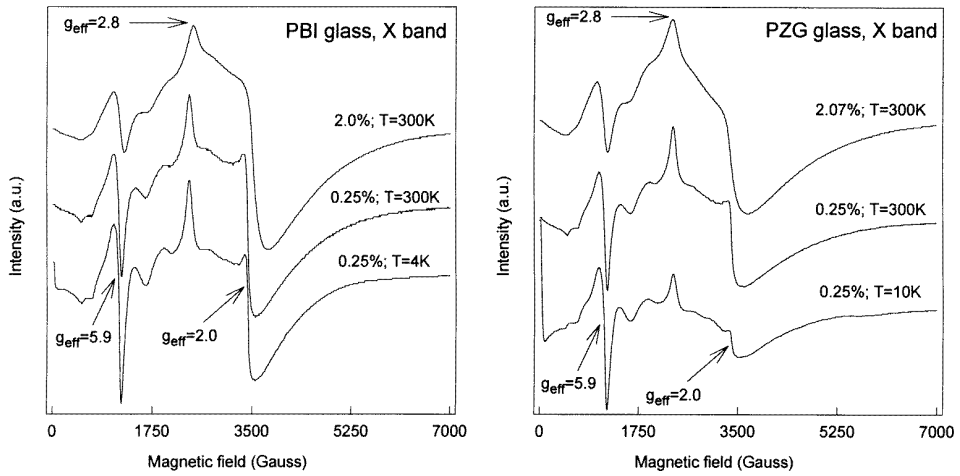

Figure 2. EPR X-band spectra of Gd^{3+} in TMFG (wt% of GdF_3): PBI glass: $\nu = 9.73$ GHz for the spectrum at the top of the figure and $\nu = 9.49$ GHz for the spectra of the lower part of the figure; PZG glass: $\nu = 9.35$ GHz for the spectrum at the top of the figure and $\nu = 9.37$ GHz for the spectra of the lower part.

At low temperature and concentration, a narrow resonance is observed at X band near zero field which gives evidence for a decrease of the absorption signal near $H = 0$. It indicates that absorption occurs for low magnetic field values [3]. Therefore, it confirms that the U-spectrum absorption curve has significant absorption dispersed through the low-field region $2.0 \leqslant g \leqslant \infty$ [1].

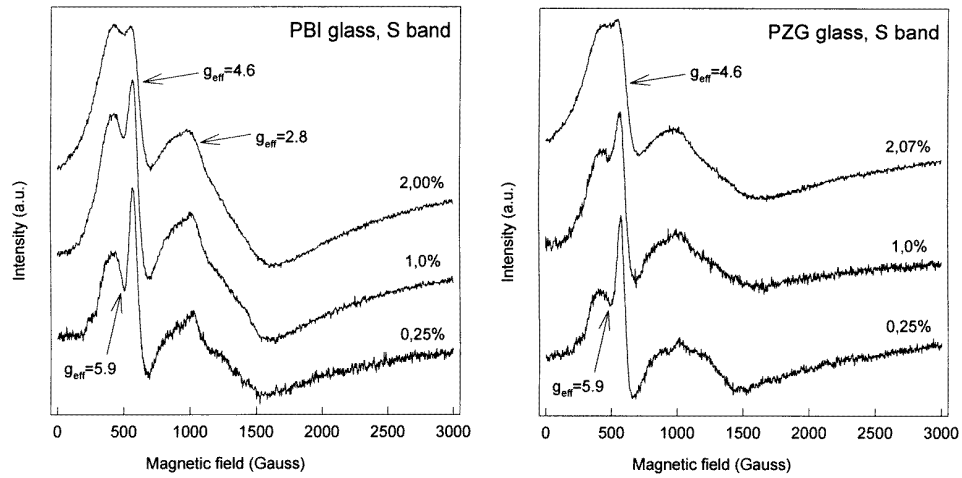

Figure 3. EPR S-band spectra of Gd^{3+} in TMFG (wt% of GdF_3): PBI glass: $\nu = 4.06$ GHz; PZG glass: $\nu = 4.05$ GHz.

At S band (figure 3), the intensity of the broad line at $g \approx 2$ and the $g_{eff} = 5.9$ to $g_{eff} = 4.6$ amplitude ratio decrease with concentration. As low-temperature experiments

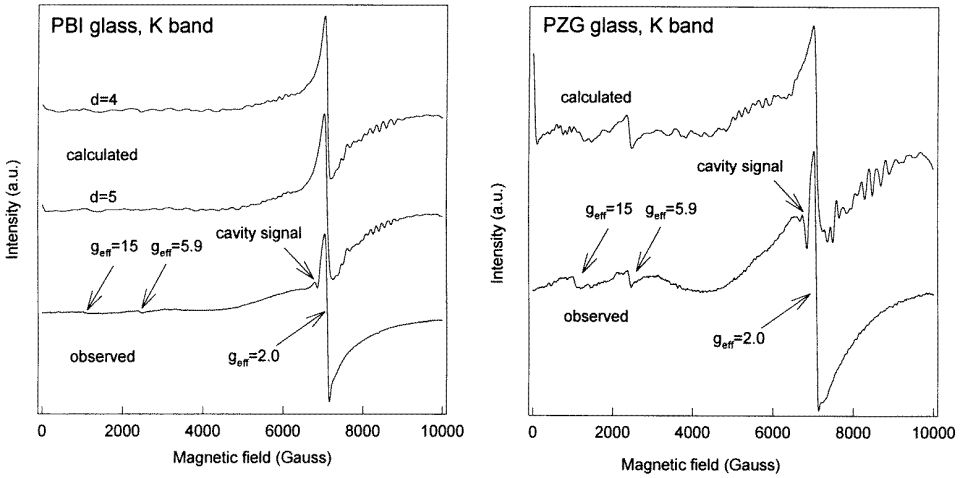

Figure 4. Observed and calculated EPR K-band spectra of Gd^{3+} in TMFG: PBI glass, $T = 12$ K, 0.25 wt% of GdF_3, $\nu = 19.8$ GHz; PZG glass, $T = 4$ K, 0.25 wt% of GdF_3, $\nu = 19.7$ GHz.

are not achievable at S band, the reader may keep in mind that the S-band spectra consist of the superimposition of pairs and isolated ion contributions. Nevertheless, the low-field resonances ($g_{eff} = 5.9$, $g_{eff} = 4.6$, and $g_{eff} = 2.8$) can be attributed to isolated ions.

3.2. Fine-structure parameter estimation

When the microwave frequency increases, an enhancement of the $g = 2$ resonance intensity is observed, whereas the low-field resonance intensity decreases.

(i) At S band ($h\nu \approx 0.135$ cm^{-1}, figure 3), all of the spectra are dominated by two low-field features with $g_{eff} = 5.9$ and $g_{eff} = 4.6$ and a broad resonance in the range 1000–1500 G.

(ii) At X band ($h\nu \approx 0.32$ cm^{-1}, figure 2), the spectra are characterized by three prominent features with effective g-values of ∼5.9, 2.8 and 2.0.

(iii) At K band ($h\nu \approx 0.66$ cm^{-1}, figure 4), the $g_{eff} = 2.8$ resonance is suppressed. A weak line is observed at $g_{eff} = 15$.

(iv) At Q band (not shown, $h\nu \approx 1.13$ cm^{-1}), there is a single nearly symmetric line at $g_{eff} = 2.0$.

When the microwave quantum is small compared with the crystal-field term, energy absorption is observed only between Kramers-conjugate states giving prominent features at certain well defined g-values; they mainly occur for $g > 2$. EPR absorption near zero magnetic field can only occur when the microwave quantum is as large as some of the crystal-field splittings. When the microwave quantum is larger than the crystal-field terms, EPR transitions will be concentrated close to $g = 2$, corresponding to the relation rule $\Delta M_S = \pm 1$.

Our results indicate therefore that most crystal-field splittings for Gd^{3+} ions in TMFG are small compared with the K- (and consequently Q-) band quantum and larger than the S-band one. The X-band spectra, with appreciable zero-field absorption and strong features at $g = 2.8$ and 5.9, indicate that there are crystal-field splittings of similar or larger magnitude

than the X-band quantum; the feature at $g_{eff} = 2.0$ indicates the existence of small crystal-field splittings compared with the X-band quantum.

Thus, from the microwave frequency dependence of the experimental spectra, we may assume that the b_2^0-distribution ranges between 0.02 and 0.15 cm^{-1}.

3.3. The glass composition dependence

At X and K bands, the amplitude ratio of the low-field ($g_{eff} = 5.9$ and 15) to $g_{eff} = 2.0$ resonance is higher for PZG. At S band, in addition to the $g_{eff} = 5.9$ and $g_{eff} = 4.6$ resonances, the PBI spectra exhibit a line at $g_{eff} = 2.8$. Moreover, the PZG spectrum differs from the PBI spectrum by a larger overlapping of the $g_{eff} = 5.9$ and $g_{eff} = 4.6$ resonances.

These observations suggest that Gd^{3+} ions occupy significantly different sites in these two glasses.

4. EPR spectrum reconstruction; determination of the fine-structure parameter distribution

The computer procedure used for line-shape calculation has been previously presented for Cr^{3+} and Fe^{3+} spectra [3]. The only difference lies in the matrix generated from the Hamiltonian (1), which is an 8×8 matrix for Gd^{3+}.

This computer spectrum calculation differs from the one used by Brodbeck and Iton in two points [1, 3], as detailed below.

(i) In our procedure, each resonance is assigned a derivative linear combination of Gaussian and Lorentzian lines, and the integrations (over magnetic field orientation and the crystal-field parameter distribution) are performed by means of the Gauss–Legendre method. Brodbeck and Iton assigned to each resonance a Gaussian absorption line, and a glassy-type spectrum was computed by summing these discrete lines and by first differentiating the absorption spectrum.

(ii) We take into account the line-width anisotropy. The transition width is calculated from the relation $L = L_0 + \Delta L$; L_0 is the isotropic line-width and $\Delta L = k(\partial H/\partial\theta)\Delta\theta$ is the anisotropic part of the line-width, where k is an adjustable parameter (the same for all calculated spectra).

In order to establish comparisons between the Brodbeck and Iton distribution and the $P(b_2^0, \lambda)$-distribution, we have performed calculations with our computer program (whose efficiency has been established in Cr^{3+} and Fe^{3+} EPR spectra simulations) for both distribution types.

4.1. The $P(b_2^0, \lambda)$-solution

An increase of d induces a shift of the $P(b_2^0, \lambda)$-maximum to higher b_2^0-values; an increase of σ induces a shift of the $P(b_2^0, \lambda)$-maximum to higher b_2^0-values and a broadening of the distribution. Thus, appreciable alterations in calculated spectrum trends (e.g. variation of the main resonance intensity ratio) are induced by σ- and d-variations.

By the trial-and-error method with integer d-values, a simultaneous agreement at any frequency is obtained, as described below.

(i) For PBI, with two sets (σ, d): $\sigma = 0.041$ (± 0.002) cm^{-1}, $d = 4$; and $\sigma = 0.033(\pm 0.002)$ cm^{-1}, $d = 5$ (figure 5). The highest probability values are observed for

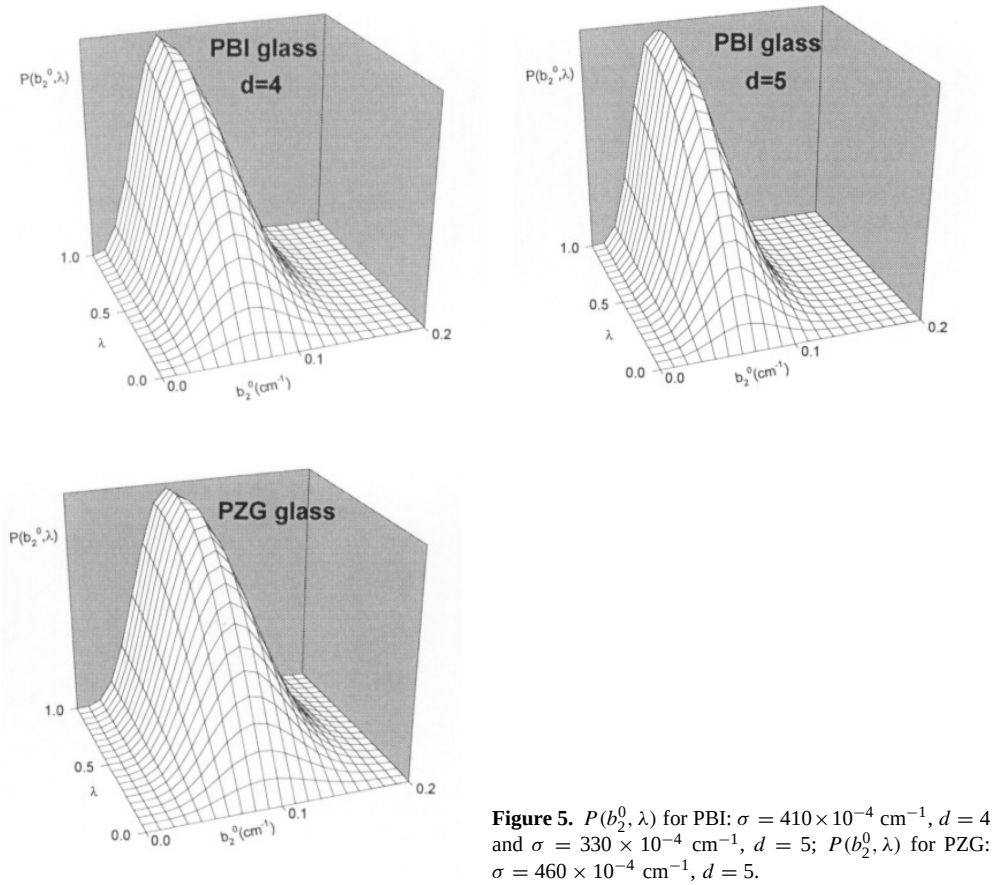

Figure 5. $P(b_2^0, \lambda)$ for PBI: $\sigma = 410 \times 10^{-4}$ cm^{-1}, $d = 4$ and $\sigma = 330 \times 10^{-4}$ cm^{-1}, $d = 5$; $P(b_2^0, \lambda)$ for PZG: $\sigma = 460 \times 10^{-4}$ cm^{-1}, $d = 5$.

the same b_2^0-values. The two distributions differ slightly from one another in width. There might be a frequency value (between S and X bands or X and K bands) which would allow one to calculate different spectra and then to determine the Gd^{3+} fine-structure parameter distribution in PBI. Nevertheless, the solution might also be either a linear combination of these distributions or a distribution characterized by σ- and d-parameters such as $0.034 < \sigma(\text{cm}^{-1}) < 0.043$ and $4 < d < 5$.

(ii) For PZG with a single set (σ, d): $\sigma = 0.046(\pm 0.004)$ cm^{-1}, $d = 5$ (figure 5).

Calculated spectra are shown in figures 4, 6 and 7. The Landé tensor value (considered as isotropic on average), the number of poles (n) used for Gauss–Legendre integration and the isotropic line-width are listed below:

$g = 1.99$ $\quad n(b_2^0) = 39$ $\quad n(b_2^2) = 39$ $\quad n(\theta) = 29$ $\quad n(\varphi) = 29$

S band: $L_0 = 40(\pm 10)$ G $\quad$ X and K bands: $L_0 = 60(\pm 20)$ G.

The computing time ranged between 90 and 200 hours according to the frequency band on a Data General Aviion 9500 computer (core: 768 Mo).

The simulated spectra closely reproduce the frequency dependence of the experimental spectra, and the position, and the intensities of the prominent features.

For Cr^{3+} and Fe^{3+}, the same L_0-value allowed us to reconstruct the spectra whatever the frequency band [3]. For Gd^{3+}, the agreement between observed and calculated S-band

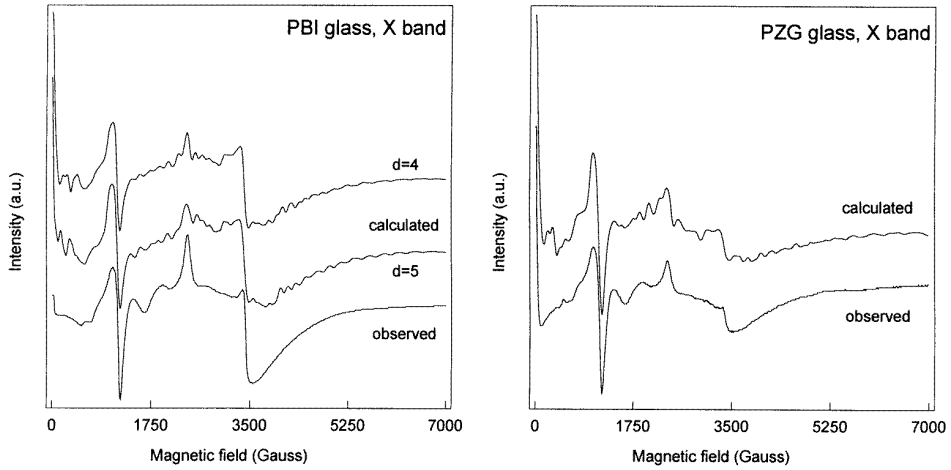

Figure 6. Observed and calculated EPR X-band spectra of Gd^{3+} in TMFG: PBI glass, $T = 4$ K, 0.25 wt% of GdF_3, $\nu = 9.49$ GHz; PZG glass, $T = 4$ K, 0.25 wt% of GdF_3, $\nu = 9.37$ GHz.

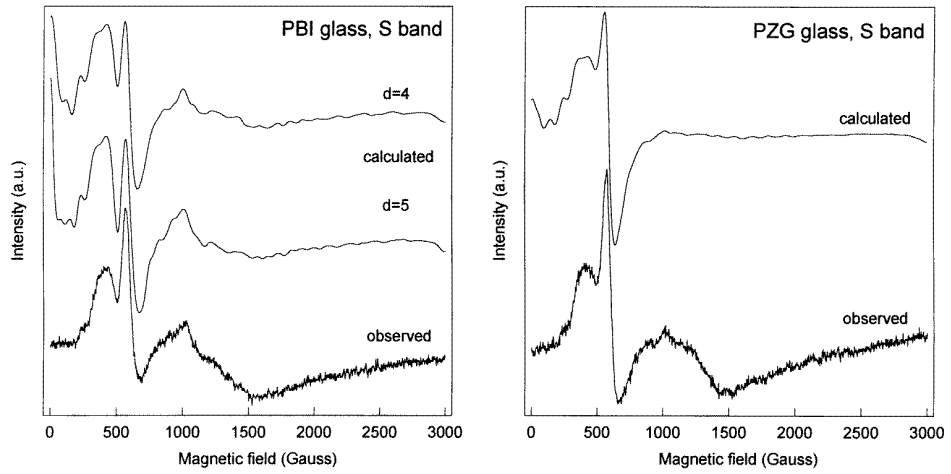

Figure 7. Observed and calculated EPR S-band spectra of Gd^{3+} in TMFG: PBI glass, $T = 300$ K, 0.25 wt% of GdF_3, $\nu = 4.06$ GHz; PZG glass, $T = 300$ K, 0.25 wt% of GdF_3, $\nu = 4.05$ GHz.

spectra is better with a weaker L_0-value. Nevertheless, owing to the uncertainty of the L_0-line-width determination, no significance is attributed to this discrepancy.

4.2. The Brodbeck and Iton solution

In order to determine the best solution to the U spectrum in the X band, Brodbeck and Iton pointed out the following line-shape characteristics: '(i) the amplitude of the peak at $g \sim 2.8$ exceeds of the positive amplitude of the $g \sim 6.0$ resonance; (ii) there is a relatively smooth dip or 'valley' in the line-shape beginning at $g \sim 2.8$ and extending to $g \sim 2.0$; and (iii)

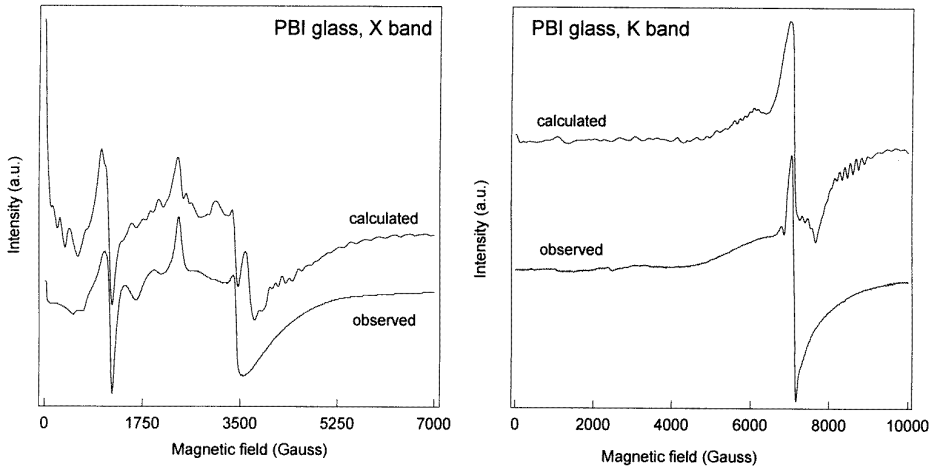

Figure 8. Observed and calculated EPR X- and K-band spectra of Gd^{3+} in PBI glass. The spectra were calculated with the Brodbeck and Iton fine-structure parameter distribution characterized by $(b_2^0)_{moy} = 0.066$ cm^{-1}, $\Delta b_2^0 = 0.019$ cm^{-1}, $\lambda_{moy} = 0.75$, and $\Delta\lambda = 2$. The Landé tensor value, the number of poles and the line-width are the same as those used for the calculation with the Czjzek distribution.

the step base-line crossing of the sharp $g \sim 2.0$ feature occurs very nearly at $g = 2.00$' [1]. From their calculations, they show that the principal features of the spectrum are taken into account accurately with a broad b_2^0-distribution with a maximum around $b_2^0 \approx 0.053$ cm^{-1}, and a broad and slowly varying λ-distribution with noticeable probability over the whole range $0 \leqslant \lambda \leqslant 1$. Obviously, our calculated spectra using Czjzek distributions do not yield characteristic (i) outlined above but satisfy fully the other two criteria in a better way than those calculated with the Brodbeck and Iton distribution. Furthermore, calculations achieved with this distribution lead to a systematically split $g = 2$ resonance (figure 15 of [1] and figure 8). This arises from sites with small λ-values which correspond to a $g = 2$ split line if b_2^0-values are sufficiently weak ($b_2^0 < 500 \times 10^{-4}$ cm^{-1} at X band and $b_2^0 < 1000 \times 10^{-4}$ cm^{-1} at K band). Thus, we may infer that the $P(b_2^0, \lambda)$-distributions, able to reconstruct accurately the $g = 2$ resonances, have to take low values for weak λ-values.

4.3. Conclusions

The Czjzek fine-structure parameter distribution allows us to obtain a better agreement between observed and calculated spectra. This solution prohibits the existence of axially symmetric sites which are difficult to expect in glasses. A Czjzek fine-structure parameter distribution is a correct general solution to the U spectrum; the alterations of the Gd^{3+} spectra on going from one glass to another can be accurately taken into account with variations of σ and d.

5. Discussion

PZG glass is a typical TMFG whose network former is built up from slightly distorted corner-sharing $(ZnF_6)^{4-}$ and $(GaF_6)^{3-}$ octahedra with Pb^{2+} at interstitial sites. The TMFG network can also be described as a mixed packing of F^- ions and large cations (Pb^{2+})

Table 1. Ionic radii (Å) for the probe and the main cations of PBI and PZG glasses (CN: coordination number).

Cation	Gd^{3+}			Zn^{2+}	Ga^{3+}	In^{3+}		Pb^{2+}		Ba^{2+}	
CN	6	8	9	6	6	6	7	8	9	8	9
Ionic radii	0.938	1.053	1.107	0.74	0.62	0.80	0.84*	1.29	1.35	1.42	1.47

* Determined from In–F distances in KIn_2F_7 [22], Sr_2InF_7 [23], $RbIn_3F_{10}$ [24], $Ba_3In_2F_{12}$ [25] and $Rb_2In_3F_{11}$ [26], where the In^{3+} ion has a coordination number equal to 7 ($r(F^-) = 1.285$ Å [21]).

induced by the vicinity of their ionic radii, with transition metal ions in octahedral holes. The structural disorder is then the result of the random character of the packing and of the wide diversity of the smaller cation sites. The Pb^{2+} coordination number is of the order of 9 [18–20]. The large size of Gd^{3+} ions is more consistent with interstitial site occupancy (with coordination number around 9, as for Pb^{2+} ions) than with octahedral hole occupancy (table 1 [21]).

PBI glass contains a larger proportion (51 mol%) of big ions, especially Pb^{2+} and Ba^{2+} (coordination number larger than (or equal to) 8), than PZG (40 mol%). Moreover, in a fluoride medium, even if the most common In^{3+} coordination number is 6, a coordination number equal to 7 is not so unusual [22–26]. Thus, the PBI network cannot be described like the PZG one. The F^- packing density is lower in PBI than in PZG; the number of polyhedra with a coordination number higher than 6 is larger. Furthermore, BaF_n polyhedra are less distorted than PbF_n polyhedra (a lone $6s^2$ pair on Pb^{2+}). Thus, Gd^{3+} ions will substitute readily into the PBI network built up from numerous high-coordination-number less distorted polyhedra (on average). For PBI, two sets of parameters allow us to obtain simultaneous agreement at any frequency. This fact could be correlated with the existence of two types of site (Ba^{2+} and Pb^{2+}) in PBI. On the other hand, in PZG glass, Gd^{3+} sites surrounded by MtF_6 and PbF_n polyhedra are more distorted. This explains the high ratio of the low-field to $g_{eff} = 2.0$ resonance, and the fine-structure parameter values being higher than for PBI glass or other fluoride glasses (ZnF_2–BaF_2–RF_3 [8], fluorozirconate [14]). In these latter glasses, Gd^{3+} ions dispose of a larger 'choice' of less distorted sites.

The second-order spin-Hamiltonian parameters for Gd^{3+}-doped fluoride crystals are given in table 2 and compared with the distribution of fine-structure parameters in Gd^{3+}-doped TMFG. It is thought that trivalent Gd^{3+} ions substitute for trivalent rare-earth RE^{3+} or Y^{3+} cations without charge compensation in these fluoride crystals.

In Li(RE or Y)F_4 and KY_3F_{10}, the trivalent cation is surrounded by eight nearest-neighbour fluorines. In Li(RE or Y)F_4, four of these are at a distance R_1 and the remaining four at a slightly different distance R_2; the local symmetry at the trivalent cation site is $\bar{4}$. In KY_3F_{10}, the eight fluorine atoms form a quadratic antiprism (local symmetry of Y^{3+}: 4; two different Y–F distances). In REF_3 compounds, the coordination number of the cation is nine.

The highest values of $P(b_2^0, \lambda)$ are observed in TMFG for b_2^0-values ((600–700) $\times$ 10^{-4} cm^{-1} for PBI glass, (700–900) $\times$ 10^{-4} cm^{-1} for PZG glass) close to the values determined for fluoride crystals ($700\times10^{-4} < |b_2^0|$ (cm^{-1}) $< 850\times10^{-4}$). This confirms that a Gd^{3+} coordination number of the order of 8 or 9 is likely for TMFG. The constituent REF_n polyhedra of these crystals are slightly distorted (weak or zero b_2^2-values) in comparison with GdF_n polyhedra in TMFG (higher probabilities observed for $0.6 < \lambda < 1$, and broad fine-structure parameter distribution with significant probability values in the ranges (300–

Table 2. Gd^{3+} second-order spin-Hamiltonian parameters b_2^m (10^{-4} cm^{-1}) in fluoride crystals and for PZG and PBI glasses (highest $P(b_2^0, \lambda)$-values).

Compound	Reference	RE^{3+} site symmetry	Coordination number	b_2^0	b_2^2
LaF_3	[27]	2	9	703	−84
CeF_3	[27]	2	9	742	−56
PrF_3	[27]	2	9	784	−82
NdF_3	[27]	2	9	812	−150
$LiYF_4$	[28]	$\bar{4}$	4 + 4	−827	
$LiDyF_4$	[29]	$\bar{4}$	4 + 4	−785	
$LiErF_4$	[29]	$\bar{4}$	4 + 4	−787	
$LiYbF_4$	[30]	$\bar{4}$	4 + 4	−838	
KY_3F_{10}	[31]	4	4 + 4	816	
PZG glass	This work		8–9*	600–700	600–700
PBI glass	This work		8–9*	700–900	700–900

* The usual coordination number in a fluoride medium.

1000) × 10^{-4} cm^{-1} for PBI and (400–1200) × 10^{-4} cm^{-1} for PZG).

The EPR spectra reconstruction in PZG and PBI glasses leads to a d-value for Gd^{3+} ($d = 4$–5) higher than those obtained for Cr^{3+} and Fe^{3+} ($d = 3$ [3]). The Gd^{3+} coordination number is larger than 6 and is variable from site to site in PZG and PBI glasses. As the coordination number increases, the number of geometrical constraints is reduced and the number (d) of independent parameters describing the fine-structure tensor becomes larger. This shows up the d-parameter sensitivity to structural constraints, and allows us to confirm the assumptions made by Czjzek in order to take into account geometrical constraints [2].

6. Conclusion

We have shown that a single distribution of crystal-field parameters, $P(b_2^0, \lambda)$, initially applied by Czjzek to the calculation of the electric field gradient in amorphous materials [2] and previously used to reconstruct Cr^{3+} and Fe^{3+} EPR spectra for TMFG [3], allows us to take into account the essential features of Gd^{3+} EPR spectra for TMFG, and to reconstruct these spectra accurately.

The agreement between observed and calculated spectra seems to be better than with the distribution proposed by Brodbeck and Iton [1], which is generally considered as the only solution for the U spectrum [9–11, 13–14]. In contrast to this previous interpretation, the distribution $P(b_2^0, \lambda)$ yields zero probability for $\lambda = 0$. From a structural point of view, this solution is more plausible. Therefore, the Czjzek distribution seems to be close to the general solution for the U spectrum which is typical of Gd^{3+} in glassy systems.

The increase of the number of independent random variables, d, in comparison with that of Cr^{3+} and Fe^{3+} ions, indicates a decrease of the number of geometrical constraints. This result is in agreement with Gd^{3+} coordination numbers being higher and variable from site to site for TMFG.

Even if the glass network imposes virtually no specific or narrowly defined site symmetries on the Gd^{3+} ions [1], the observed changes as functions of glass composition show that the glass network has an influence on the polyhedra distortion amplitude of Gd^{3+} ions.

Acknowledgment

The authors acknowledge P Simon (CRPHT UP CNRS 4212) for recording the Q-band spectrum.

References

[1] Brodbeck C M and Iton L E 1985 *J. Chem. Phys.* **83** 4285
[2] Czjzek G, Fink J, Götz F, Schmidt H, Coey J M D, Rebouillat J P and Liénard A 1981 *Phys. Rev.* B **23** 2513 Czjzek G 1982 *Phys. Rev.* B **25** 4908
[3] Legein C, Buzaré J Y, Emery J and Jacoboni C 1995 *J. Phys.: Condens. Matter* **7** 3853
[4] Jacoboni C, Le Bail A and De Pape R 1983 *Glass Technol.* **24** 164
[5] Auriault N, Guery J, Mercier A M, Jacoboni C and De Pape R 1985 *Mater. Res. Bull.* **20** 309
[6] Berlinger W and Müller K A 1977 *Rev. Sci. Instrum.* **48** 1161
[7] Cugunov L and Kliava J 1982 *J. Phys. C: Solid State Phys.* **15** L933
[8] Yoneda Y, Kawazoe H and Kanazawa T 1983 *J. Non-Cryst. Solids* **56** 33
[9] Rao A S, Rao J L, Kumar V V R K, Jayasankar C K and Lakshman S V K 1992 *Phys. Status Solidi* b **174** 183
[10] Ramana M V, Lakshmi P S, Sivakumar K, Sathyanarayan S G and Sastry G S 1991 *Phys. Status Solidi* a **126** K181
[11] Badets M C, Simon P, Rifflet J C and Coutures J P 1989 *Mater. Res. Bull.* **24** 483
[12] Nicklin R C, Johnstone J K, Barnes R G and Wilder D R 1973 *J. Chem. Phys.* **59** 1652
[13] Venkatasubbaiah A, Sreedhar B, Rao J L, Lakshman S V J and Kojima K 1994 *Mater. Res. Bull.* **29** 911
[14] Furniss D, Harris E A and Hollis D B 1987 *J. Phys. C: Solid State Phys.* **20** L147
[15] Griscom D L 1980 *J. Non-Cryst. Solids* **40** 211
[16] Iton L E and Turkevich J 1977 *J. Chem. Phys.* **81** 435
[17] Legein C, Buzaré J Y and Jacoboni C 1993 *J. Non-Cryst. Solids* **161** 112
[18] Le Bail A, Jacoboni C and De Pape R 1985 *Mater. Sci. Forum* **6** 441
[19] Boulard B, Jacoboni C and Rousseau M 1989 *J. Solid State Chem.* **80** 17
[20] Legein C, Buzaré J Y, Boulard B and Jacoboni C 1995 *J. Phys.: Condens. Matter* **7** 4829
[21] Shannon R D 1976 *Acta Crystallogr.* A **32** 751
[22] Champarnaud-Mesjard J C and Frit B 1977 *Acta Crystallogr.* B **33** 3722
[23] Scheffler J and Hoppe R 1984 *J. Fluorine Chem.* **25** 27
[24] Champarnaud-Mesjard J C, Mercurio-Lavaud D and Frit B 1977 *J. Inorg. Nucl. Chem.* **39** 947
[25] Hoppe R and Scheffler J 1985 *Z. Anorg. Allg. Chem.* **521** 79
[26] Champarnaud-Mesjard J C and Frit B 1978 *Acta Crystallogr.* B **34** 736
[27] Misra S K, Mikolajczak P and Lewis N R 1981 *Phys. Rev.* B **24** 3729
[28] Vaills Y, Buzaré J Y and Gesland J Y 1983 *Solid State Commun.* **45** 1093
[29] Misiak L E 1993 *Acta Phys. Pol.* A **83** 195
[30] Misiak L E, Misra S K and Mikolajczak P 1988 *Phys. Rev.* B **38** 8673
[31] Debaud-Minorel A M, Mortier M, Buzaré J Y and Gesland J Y 1995 *Solid State Commun.* **95** 167